AUTOMATIC ROOF MODEL RECONSTRUCTION USING THE TIN-MERGING AND RESHAPING ALGORITHM

Po-Chia Yeh[1] and Jiann-Yeou Rau[2]
[1] Graduate Student, Department of Geomatics, National Cheng Kung University, No.1 University Road, Tainan City, Taiwan; Tel: (886)6-2757575 Fax: (886)6-2375764;
Email: nowitzki100@gmail.com

[2] Assistant Professor, Department of Geomatics, National Cheng Kung University, No.1 University Road, Tainan City, Taiwan; Tel: (886)6-2757575 Fax: (886)6-2375764;
Email: jyrau@mail.ncku.edu.tw

KEY WORDS: Cyber-city, Roof Model Reconstruction, Topology Reconstruction, TIN-Merging and Reshaping

ABSTRACT: Three-dimensional building model is one of the major components of a cyber-city and is vital for the realization of 3D GIS applications. Related researches can be categorized into "data-driven", "model-driven" and hybrid approaches. The data used could be high-resolution satellite imagery, airborne stereo-pairs, airborne laser scanning, or combination of these data using data fusion scheme. This paper presents a novel algorithm for automatic reconstruction of roof models from 3D structural lines of a building, i.e. their eaves and ridges, which are measured from aerial stereo-pairs. A line-based roof model reconstruction algorithm, namely TIN-Merging and Reshaping (TMR), is proposed. The originality for 3D roof modeling is to perform geometric analysis and topology reconstruction and then reshapes the roof using elevation information from the original 3D structural lines. The proposed scheme reduces the complexity of 3D roof modeling and makes the modeling process easier. The final 3D polyhedral building models are generated by interpolating the building foot height from a digital elevation model. One test area was conducted covering university campus and residential area. Experimental results indicate a nearly 100% success rate for topology reconstruction can be achieved provided that the 3D structural lines can be enclosed as polygons. However, the success rate of the Reshaping stage is dependent on the complexity of the rooftop structure. The results demonstrate that the proposed scheme is robust and accurate, with a high degree of automation, even when a group of connected buildings with multiple layers and mixed roof types is processed.

1. INTRODUCTION

Three-dimensional building model is one of the major components of a cyber-city and is vital for the realization of 3D GIS applications. The building model is essential for true-orthophoto generation (Rau et al., 2002), map revision, change detection, energy and property management, micro-climate and air pollution simulations, and many location-based services. In a photo-realistic city model, geometric building models are also required for the generation of façade and rooftop texture. Such models can be applied in virtual city tourism, urban planning, real-estate markets, smart cities, among others. The generation of reliable and accurate 3D building models is crucial to accomplish the above mentioned goals.

Generally, the procedure for geometrical building modeling or city modeling encompasses three main steps, namely (1) recognition, (2) feature extraction, and (3) topology reconstruction with geometric modeling. Rather than automatic recognition, the most reliable and accurate results can normally be achieved by a building reconstruction system that integrates human-assisted visual interpretation capability (Gruen and Wang, 1998). For a fully autonomous system, the integration of multiple data sources, such as multiple aerial images, ALS data, and 2D ground plans, might increase the reliability and degree of automation, but some constraints or limitations in certain aspects are unavoidable. Examples include the capability of handling a high density of built-up areas, occlusions from trees or neighboring buildings, bad image quality due to shadows, weather conditions or digitized imagery, insufficient image resolution or point clouds density, miscellaneous objects on the rooftop, etc. (Baillard and Zisserman, 2000; Brenner, 2000; Elberink and Vosselman, 2009).

The purpose of feature extraction is to retrieve 3D primitives of building structure from images or laser scanning data, including corners, ridges, eaves, faces, and so on. In the case of images, further image matching is required to perform space intersection from more than two images (Baillard and Zisserman, 2000). Canny and Förstner operators are the two most commonly used methods in Computer Vision and Digital Photogrammetry for the purpose of extracting point- or line-based features, while the Hough Transform is often used for straight line detection after feature point detection.

In this study, we assume that the roof patches can be described by several planar regions and enclosed by roof structural lines digitized by manual stereo-measurement of a stereo-pair. An algorithm based on the derived

structural lines for rebuilding roof polygons is thus proposed.

2. METHODOLOGY

The TIN-Merging and Reshaping (TMR) algorithm is comprised of four main steps. The first one is a pre-processing step to repair any measurement errors in input structural lines or imperfect results from feature extraction. This can include performing right angle rectification, line collinearity adjustment, snapping of dangles from shortening, and removal of overhanging dangles. The second step is to construct a Triangulated Irregular Network (TIN) using Constrained Delaunay Triangulation (CDT) (Chew, 1987; Kallmann et al., 2003), where the vertices of structural lines are adopted as points and the structural lines themselves are used for constraining the generated TINs. Two neighboring TINs are iteratively merged by removing the shared edges that have no corresponding structural lines. The resultant roof topology is reconstructed in a 2D projection. Finally, we reshape the roof structure based on the rectified structural lines that contain the third dimensional information (Z) to infer 3D roof models.

2.1 Pre-processing

Since the imperfect generation of structural lines is unavoidable during the feature extraction stage or during manual stereo-measurement, it is necessary to correct them before the construction of TINs; otherwise some illegal TINs will be generated. Fig. 1(a) depicts several examples of such deficiencies, in which the red lines are the measured structural lines and the blue dots denote the detected dangles. For example, a rectangular building might be skewed, structural lines might pierce a wall or be disconnected from a neighboring wall, two collinear-like lines might be distorted, multiple convergent lines might be detached, and so on. Meanwhile, when dangles exist, some illegal triangles will be generated and the topology reconstruction will fail. Thus, the pre-processing of detected lines has to be robust and rigorous in order to successfully reconstruct their topology. Fig. 1(b) shows the pre-processing results, i.e. rectified structural lines, where the dangles were removed successfully. This procedure can be performed fully automatically in the developed system after rational determination of several adopted parameters, such as θ and ρ for collinearity verification, the maximum dangle length, and the maximum rotation angle for right-angle rectification.

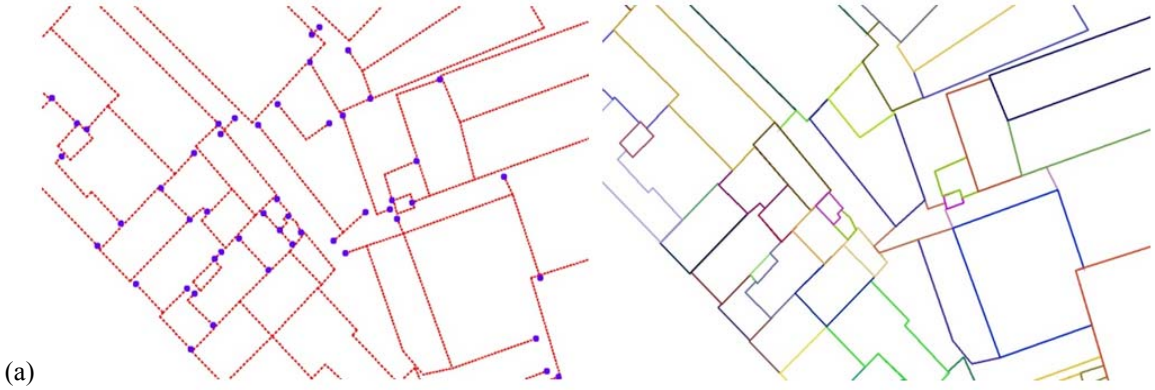

(a) (b)

Fig. 1. (a) Original measured (red) lines with dangles (blue); and (b) the generated polygons (each in a different color).

2.2 Constrained Delaunay Triangulation

Delaunay Triangulation (Delaunay, 1934) is a well-known technique for constructing triangles from sparsely distributed points where there is no fourth point inside its circumcircle to avoid spear-like triangles. Using this technique unrelated points can be organized in such a way that neighborhoods are connected with topology. Delaunay Triangulation is thus useful for topology reconstruction of unrelated points. In this study, the primitive for roof model reconstruction is derived from structural lines which have to be enclosed to define a polygon. The generated TINs cannot intersect or cross over the structural lines. The endpoints of the structural lines act as points for constructing TINs on the 2D horizontal plane but are constrained by the structural lines themselves using Constrained Delaunay Triangulation (Chew, 1987; Kallmann et al., 2003) to avoid triangles crossing the structural lines. Fig. 2 illustrates the effect with and without applying the line constraint in the generation of TINs. Fig. 2(a) shows the input lines and Fig. 2(b) shows the generated TINs without the line constraint. One may notice that some created triangles have crossed over the original lines. Fig. 2(c) illustrates the results after applying the line constraint. It is obvious that the use of the line constraint for TINs generation can achieve reasonable and correct topology.

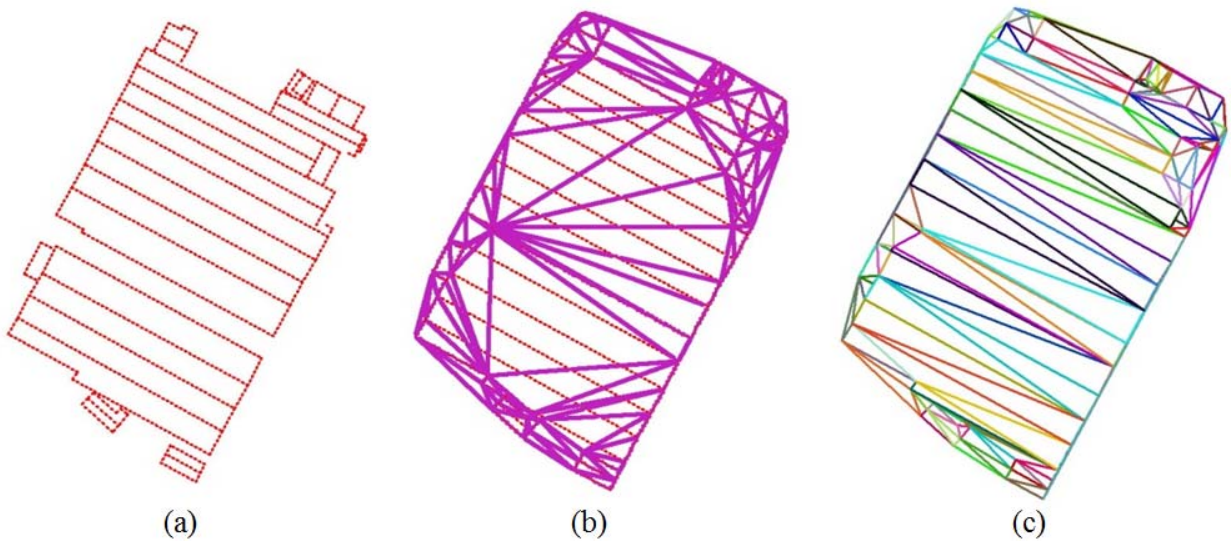

Fig. 2. Delaunay Triangulation with and without line constraint.

2.3 TIN-Merging

After the generation of TINs, the relationship among the structural lines is created. The TINs are described in convex hull. Some of them appear around concave building boundaries do not exist in the real world and should be removed in advance. Meanwhile, some shared edges between two TINs that do not exist should be eliminated as well. This can also reduce the volume of data storage and present rational roof models. The clue for the detection of existing edges is these rectified structural lines. We can merge two neighboring TINs by erasing the shared edge that has no corresponding structural line. The TIN-Merging procedure is thus an iterative loop used to check for shared edges between two TINs (or polygons) to verify whether there is any overlap or collinearity between the shared edges and the rectified structural lines. If there is no corresponding line, the shared edges will be removed and those two TINs (or polygons) are merged as one polygon.

Fig. 3 shows an example of TIN-Merging. The CDT results are shown in Fig. 3(a). Fig. 3(b) is the results after applying TIN-Merging and Fig. 3(c) shows the results after removing the outer TINs that do not exist in the real world. It can be seen in Fig. 3(c) that there is a small roof surrounded by another, thus two additional pseudo edges (same location but different directions) are added to connect each other. The edge sequence numbers are denoted. Line numbers 8 and 13 are two pseudo edges that have no corresponding structural lines but are kept to describe this donut-type polygon. Since two polygons should not overlap after topology reconstruction, the inner polygon has to be encircled by the outer one. It means that the outer polygon has to be cut by the inner one resulting in a donut-type polygon. One may compare the 3D view in Fig. 3(d) for clarification.

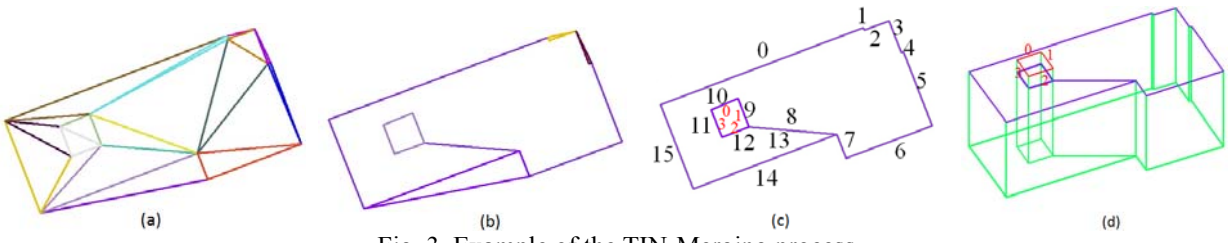

Fig. 3. Example of the TIN-Merging process.

2.4 Reshaping

Before reshaping, recalling that all the above procedures are processed in two-dimensional space. This reshaping procedure utilizes the third dimensional information (Z) from the endpoints of rectified structural line to infer the final shape of the roof structure. The basic idea behind constructing a roof shape (whether flat or inclined) from 3D lines is that two connected lines will have the same 3D coordinates at their joint and form a triangle. A triangle always located on a plane. The parameters of a planar function can thus be calculated by the vertices of the triangle.

In the beginning, all edges are classified as independent, shared or pseudo edges. The pseudo edges are created during the construction of Delaunay Triangulation as described in the previous section. An independent edge means that no neighbor polygon is connected, but a shared edge has. For example, edge numbers 9 to 12 in Fig. 3(c) are

shared edges while the other edges (with the exception of edge numbers 8 and 13) are independent edges. The height value for an independent edge can be initialized and fixed by the Z-value of its corresponding 3D line terminals. On the other hand, the height value for the shared edges and pseudo edges can only be initialized, but is not yet fixed.

At the second stage, a coplanar verification process is applied for all edges within a polygon. This step is particularly essential for a roof that is taller than its surrounding roofs. In the previous stage they are assigned as shared edges, such as the inner roof depicted in Figs. 3(c) and 3(d) highlighted by the red numbers 0 to 3. If all the edges of this polygon are located on a plane, they will be classified as independent edges with fixed heights. It is worth noting that currently edge numbers 9 to 12 in Fig. 3(c) are still remained as shared edges. On the other hand, for a gable roof, the ridge lines are first considered to be shared edges. They will be considered as independent edges by applying this coplanar verification process. Fig. 4 illustrates a gable roof (the rightmost one) and a flat roof (the leftmost one) whose shape is determined at this procedure. In the figure, the independent edges are depicted in yellow and the shared edges in white. The shape of the gable roof in the middle and the small flat roof cannot be determined in the current stage, because the initial heights of the shared edges are assigned by its neighborhood that is taller and will cause non-planar situation.

The third step of reshaping is to search for the existence of independent edges within a polygon. Once more than two independent edges are found, the least-squares adjustment can be applied to calculate the plane equation for this polygon and to determine the heights of the other shared edges. These two independent edges can be connected or parallel to each other to form a triangle or a rectangle as long as they fall on a plane. The height value of the other shared edges will be adjusted and their attribute will be reassigned as independent edges. The smaller flat roof shown in Fig. 4 is an example of this case. Since three of the edges are independent, the height of the remaining shared edge can be decided and fixed directly by least-squares adjustment.

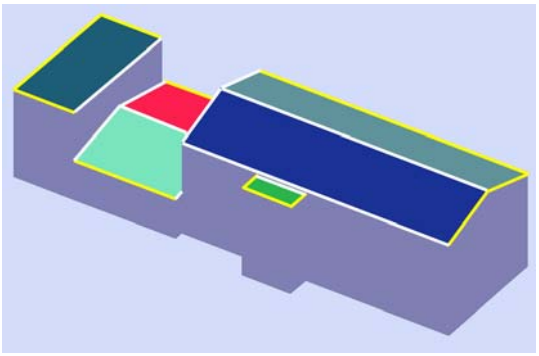

Fig. 4. Example of independent (yellow) and shared (white) edges.

3. CASE STUDY

3.1 Study area

The 3D structural lines were manually measured from a pair of aerial photographs with 60% overlap using a digital photogrammetric workstation. The photographs have a scale of 1:5,000 and were digitized with a scanner with a resolution of 25 μm which results in a nominal ground sampling distance (GSD) of 12.5 cm. The test site is located around the Fu Jen Catholic University, Taiwan. The area is about 70 hectares in size and contains more than 1000 buildings. The content of the test site can be roughly categorized into two parts. Part (I) is comprised of the university campus including mostly large and separated buildings with complex boundaries but simpler roof structures. Part (II) includes high-density buildings with groups of complex roofs where industrial factories, residential houses and apartments are located. Fig. 5 depicts the measured 3D roof structure lines on the ground projection with the university located in the upper-right region. For research purposes, most of the measured 3D structural lines are not complete. This means that due to the occlusion effect only the visible parts are measured and there can be large gaps between the roof eaves and neighboring buildings. This procedure is different from conventional stereo-mapping where the occluded eaves or corners are inferred from one of the utilized stereo-images to minimize the gap between them. There are some examples of this situation discussed in this paper.

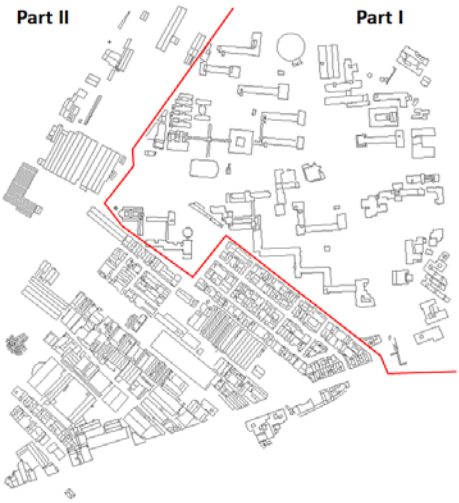

Fig. 5. Test dataset of 3D structure lines on 2D horizontal projection.

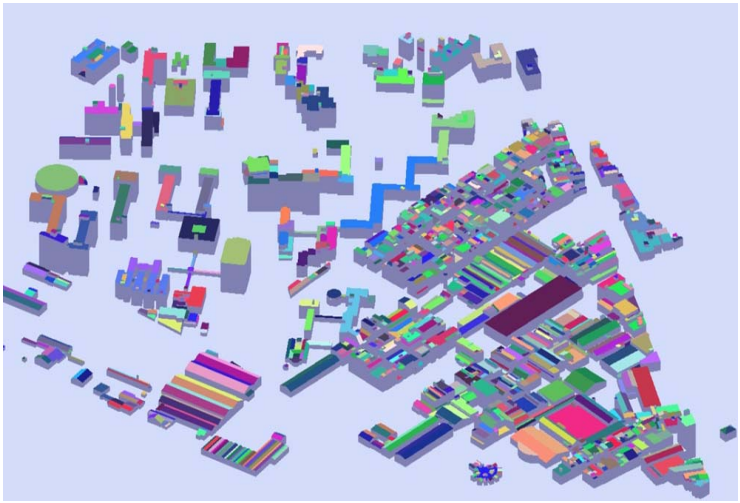

Fig. 6. Reconstructed 3D building models.

3.2. Analyses

The reconstructed 3D building models for the test dataset are illustrated in Fig. 6. The number of dangles before pre-processing was 1,542, but after dangle removal at the pre-processing stage this number was reduced to zero. This indicates that the developed pre-processing algorithm is robust and effective. The success rate for TIN-Merging topology reconstruction is close to 100%, except for the area where building boundary delineation has not been measured to enclose the roof. To sum up, the total number of 3D roof models (polygons) generated is 1,573. Nevertheless, the success rate for reshaping is dependent on the complexity of the roof structure. For buildings in the university area (Part I), the reshaping success rate can reach up to 98%, while for other areas (Part II, outside the campus) it is only 90%. The average reshaping success rate for the whole dataset is 92%. Most of the failures occurred with inclined roofs surrounded by other buildings with varied heights and roof types.

Due to the occlusion effect, the structural lines of the roofs cannot be completely measured from the stereo-image. Their endpoints are not inferred from the other visible image or edited manually. Fig. 7(a) shows an example of the measured 3D lines projected on the horizontal plane. The detected dangles are denoted as blue dots. The dangling effects are solved by applying the pre-processing steps, as shown in Fig. 7(b). The incomplete lines have been extended to reach a wall or a vertex. However, sometimes the extension from the dangle itself is not enough. Please note that the dangles depicted in the blue dashed circles closest to the wall, which has already closed with other wall, also need to be extended in order to enclose the roof boundary.

All vertices are used as 2D points and the structural lines act as constraints for the generation of Delaunay Triangulation. The results after Constrained Delaunay Triangulation are illustrated in Fig. 7(c). Several shared edges that do not exist in the real world are removed during the TIN-Merging step. As a result, the topology among these structural lines can be rebuilt and the roof polygons as well, as depicted in Fig. 7(d) with different colors. The results of reshaping the roof-top structure are shown in Fig. 7(e). Comparing Figs. 7(d) and 7(e), one may observe that the height of roof polygons A and B is the same as their neighboring polygon C. Actually, polygon C is an outdoor hallway and polygons A and B do not exist, but unfortunately the current algorithm cannot determine whether they exist or not, or whether they are lower than their neighbors, unless further auxiliary information is given, for example the ALS data.

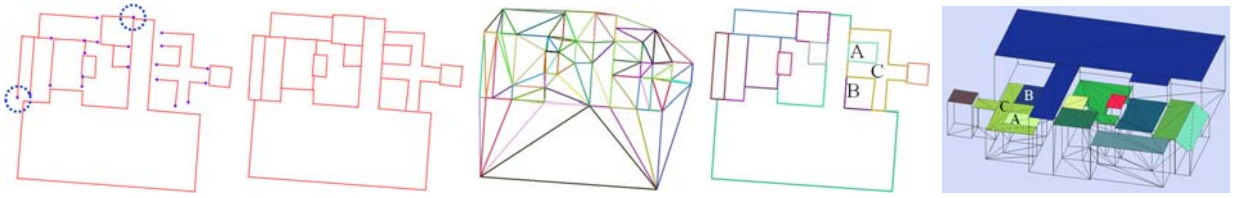

Fig. 7. From left to right: (a) Original 3D lines; (b) after dangle removal; (c) the generated Delaunay Triangulation; (d) reconstructed polygons; and (e) the generated building models.

The roof structures in the previous case are mostly flat. The reshaping step is much easier when no measurement errors exist. However, human mistakes may occur. For example, in Fig. 8 there are four gable roofs, one of which

contains a measurement mistake; more specifically is missing an eave. Thus, the inferred roof structure could be wrong. Fig. 8 shows three possible roofs based on the currently measured 3D lines, i.e., the red lines. This would be better corrected before 3D roof modeling.

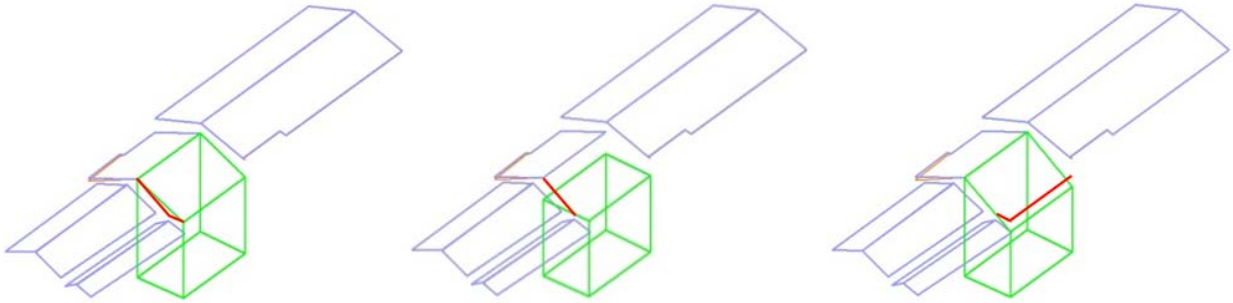

Fig. 8. Reshaping ambiguity due to measurement mistakes or complex roof structures.

5. Conclusions

This paper presents an automatic building modeling technique for complex roof based on 3D structural lines derived from stereo-plotting. An innovative line-based 3D roof modeling algorithm called TIN-Merging and Reshaping is the core to rebuild the topology between roof structure lines and reshaping the roof type. The performance evaluation shows that an almost 100% success rate can be achieved with the proposed TIN-Merging step for 2D topology reconstruction, utilizing a high degree of incomplete manually measured 3D structural lines, provided that the roof boundary are well enclosed. However, the success rate for reshaping depends on the complexity of the roof structure. A 98% reshaping success rate is observed for buildings located within the university, where the buildings are large and their roof structures simpler. However, the success rate is only 90 % for an area with mixed residential and industrial buildings where the roofs are mostly small and surrounded by others with great variation in height and roof type. The accuracy of the generated 3D roof models is decided at the stage of manual stereo-plotting. The proposed algorithm is a line-based 3D roof modeling procedure which is suitable for integrating with digital photogrammetry workstation and topographic mapping.

ACKNOWLEDGEMENTS

This research was financially supported by the National Science Council, Taiwan (Project # NSC 96-2628-E-006 -257 -MY3). The authors are grateful to Prof. L.C. Chen of the Center for Space and Remote Sensing Research, NCU, Taiwan, for providing valuable advice and test data. Many thanks also go to Mr. Bo-Cheng Lin for his assistance in programming.

REFERENCES

Baillard, C., and Zisserman, A., 2000 . "A plane-sweep strategy for the 3D reconstruction of buildings from multiple images." International Archives of Photogrammetry and Remote Sensing, 33, B2; PART 2, 56–62.

Brenner, C., 2000. "Towards fully automatic generation of city models." International Archives of Photogrammetry and Remote Sensing, 33, B3/1; PART 3, 84–92.

Chew, L. P. , 1987. "Constrained delaunay triangulations." Proceedings of the third annual symposium on Computational geometry, Waterloo, Ontario, Canada, 215-222.

Delaunay, B., 1934. "Sur la sphère vide, Izvestia Akademii Nauk SSSRSur la sphère vide, Izvestia Akademii Nauk SSSR." Otdelenie Matematicheskikh i Estestvennykh Nauk, 7, 793-800.

Elberink, S. O., and Vosselman, G., 2009. "Building reconstruction by target based graph matching on incomplete laser data: analysis and limitations." Sensors, 9, 6101-6118.

Gruen, A., and Wang, X., 1998. "CC-Modeler : a topology generator for 3-D city models 1." ISPRS Journal of Photogrammetry & Remote Sensing, 53, 286-295.

Kallmann, M., Bieri, H., and Thalmann, D., 2003. "Fully dynamic constrained delaunay triangulations." In Geometric Modelling for Scientific Visualization, G. Brunnett, B. Hamann, H. Mueller , Eds. , Springer-Verlag, 241-258.

Rau, J. Y., Chen, N. Y., and Chen, L. C., 2002. "True orthophoto generation of built-up areas using multi-view images." Photogrammetric Engineering and, 68, 6, 581-588.